

Analysis of inflammatory periimplant lesions during a 12-week period of undisturbed plaque accumulation—a comparison between flapless and flap surgery in the mini-pig

Cornelia K. Mueller · Michael Thorwarth ·
Stefan Schultze-Mosgau

Received: 16 July 2010 / Accepted: 9 March 2011 / Published online: 29 March 2011
© Springer-Verlag 2011

Abstract This study's aim was to clarify the influence of soft tissue management on the development of periimplant infection. Four weeks after removal of all maxillary premolars in 12 mini-pigs, four BEGO Semados RI implants were inserted in each maxillary quadrant. Employing a split-mouth design, one quadrant was randomized to flapless insertion while the contralateral side was chosen for flap surgery. Following 1, 2, 4 and 12 weeks of transmucosal implant, healing biopsies were retrieved from the periimplant soft tissue and subjected to further analysis. Histomorphometrically, a significant reduction of transmigration of polymorphonuclear neutrophils (week 1, $p=0.007$; week 2, $p=0.021$; week 4, $p=0.023$; week 12, $p=0.013$) as well as the density of the subepithelial inflammatory infiltrates (week 1, $p=0.007$; week 2, $p=0.046$; week 4, $p=0.003$; week 12, $p=0.032$) was verified following flapless surgery. Quantification of inducible nitric oxide synthase showed significantly reduced expression in the flapless group 2 ($p=0.027$), 4 ($p=0.005$) and 12 ($p=0.004$) weeks post-insertion. Analysis of CD31 and collagen I immunostained sections revealed more regular capillary distribution as well as higher vessel and collagen density in the flapless group. The data of the present study indicate that flapless placement reduces the incidence of inflammatory periimplant soft tissue lesions during a 12-week period.

Considering the beneficial effects of flapless placement on early soft tissue healing and stability, the technique might be preferred in case of an uncomplicated locoregional anatomy with sufficient hard and soft tissue. However, this positive effect might disappear after manipulation of the implant and soft tissue during impression taking or try in of the prosthodontic supraconstruction.

Keywords One-stage implant surgery · Flapless placement · Periimplant inflammation

Introduction

At the moment, most practitioners prefer to insert their implants after soft tissue flap elevation to visualize better the bone sites where the implants will be placed and thus minimize the risk of bone perforation or incorrect implant alignment [1]. Besides standard flap surgery, minimally invasive flapless placement, exposure of the alveolar crest by a tissue punch or a stab incision [2], has been introduced for a broad spectrum of indications, especially in conjunction with the techniques of computed tomography/dental volume tomography based-guided surgery [3].

In a parallel group design, randomized controlled trial Fortin et al. found significantly reduced postoperative pain and analgesic intake following flapless surgery as compared with the flap procedure in the 6-day follow-up [4]. Reduced postoperative pain, analgesic consumption and less edema following flapless procedures were confirmed by another randomized controlled trial conducted by Cannizzaro et al. [5]. Furthermore, a recent review summarized that there is evidence suggesting that flapless surgery causes less postoperative pain, edema and consumption of analgesics than conventional flap elevation. However, insufficient

C. K. Mueller · M. Thorwarth · S. Schultze-Mosgau
Department of Oral and Maxillofacial Surgery/Plastic Surgery,
School of Medicine, University of Jena,
Jena, Germany

C. K. Mueller (✉)
Department of Oral and Maxillofacial Surgery/Plastic Surgery,
Friedrich-Schiller-University,
Erlanger Allee 101,
07747 Jena, Germany
e-mail: Cornelia.Mueller1@med.uni-jena.de

evidence exists regarding the influence of flapless placement on the incidence of periimplant infectious lesions and the potential increased risk of complications/failures using a flapless approach [6].

A series of histologic studies using a mongrel dog model was initiated to investigate the influence of the insertion technique on periimplant soft tissue consolidation. You et al. found significantly reduced height of the periimplant mucosa, length of the junctional epithelium, gingival index, bleeding on probing, probing depth and marginal bone loss 3 months after flapless placement as compared with flap surgery [7]. Furthermore, significantly more blood vessels were found in the supracrestal connective tissue 3 months after flapless insertion [8]. Furthermore, in a dog model as well as a clinical study, Jeong et al. were able to demonstrate that flapless surgery enhances the process of osseointegration and reduces the amount of crestal bone loss [9, 10].

Taking into account the previous results on the effect of flapless placement on periimplant soft tissue consolidation and the lack of evidence regarding its influence on the incidence of periimplant infectious lesions, the aim of the present mini-pig study was to test the following hypothesis:

1. Flapless surgery reduces the amount of periimplant inflammation and infection measured as the number of transmigrated polymorphonuclear neutrophils (PMNs) in the junctional epithelium, the density of subepithelial inflammatory infiltrates as well as the expression of the inducible nitric oxide synthase (iNOS).
2. Flapless surgery enhances the vessel density and collagen I deposition in the supracrestal connective tissue.

Materials and methods

Study design

The study protocol was approved by the Thuringian State Office for Food Safety and Consumer Care (registration number: 02-028/06). A total of 12 female miniature pigs, 12 months of age with an average body weight of approximately 35 kg (Ellegard Goettinger Mini-pigs, Dalmose, Denmark) was used for the investigations. The mini-pig was chosen as it is established as a model for periimplant osseous and soft tissue healing under clinically relevant conditions [11].

Employing an early implant placement approach 4 weeks after removal of all premolars from each maxillary quadrant, four BEGO Semados RI titanium implants (4.1 × 10 mm, BEGO Implant Systems, Bremen, Germany) were inserted in each maxillary quadrant in all animals

(four per side, eight per animal). Employing a split-mouth design, one maxillary quadrant was randomized to flapless insertion while the contralateral side was chosen for conventional flap surgery. Following 1, 2, 4 and 12 weeks of transmucosal implant healing, biopsies were retrieved from the periimplant soft tissue and subjected to standard histology, histomorphometry, real-time reverse transcriptase-polymerase chain reaction (RT-PCR), immunofluorescence and immunohistochemistry.

Anesthesia and surgical protocol

After overnight fasting with free access to water, the pigs were premedicated with ketamine (10 mg/kg body weight, Ketavet®; Pharmacia & Upjohn, Erlangen, Germany) and midazolam (1 mg/kg body weight, Dormicum®; Ratiopharm, Ulm, Germany) to allow placement of an intravenous line in the ear vein. General anesthesia was induced with propofol (30 mg/animal, Fresenius Kabi, Bad Homburg, Germany). Then the trachea was orally intubated with an endotracheal tube and anesthesia was maintained with isofluran (Baxter, Heidelberg, Germany). The implantation site was disinfected carefully with 0.2% chlorhexidine solution (GlaxoSmithKline, Munich, Germany). For local control of bleeding articain 4% cum 1:100,000 epinephrine (Ultracain D-S forte®; Sanofi Aventis Dt. GmbH, Frankfurt, Germany) was administered to the implantation site.

For flapless insertion, a mucosal punch with a trephine drill was used to expose the alveolar crest. According to the recommendations of Choi and Engelke [1], the punch diameter was undersized compared with the healing abutment ($\varnothing_{\text{punch}}$ 4.1 mm vs. $\varnothing_{\text{healing abutment}}$ 5 mm) to facilitate proper soft tissue adaption. To perform open surgery, a paracrestal, slightly palatally displaced, incision without releasing incisions was made and the mucoperiosteum was elevated buccally and orally to expose the alveolar crest.

Implant beds were prepared using spiral drills with increasing diameter and a screw tapper according to the manufacturer's protocol. To achieve reproducible coronal implant positioning, a 10 mm-drill stop was employed on bone level. In order to adjust for the overlying soft tissue in the flapless group, mucosal thickness was determined and the individual value was added to the predefined 10-mm drilling depth. The torque during implant insertion was adjusted to ≤ 45 Ncm. Following insertion implants were covered with the corresponding titanium healing abutments (BEGO Implant Systems). For the open protocol, resective counteracting of the buccal flap was performed to facilitate circumferential adaption of the soft tissue around the emerging implant structures. The countered flap was then coronally repositioned and secured around the healing abutments with interrupted, non-

resorbable, 3–0 sutures (Ethilon; Ethicon, Norderstedt, Germany) passing through each interimplant area. The mini-pigs were maintained on a soft diet for 2 weeks post-implantation and fed a normal diet (Altromin 9023; Lage, Germany) until the end of the study. To prevent infection, the pigs were given enrofloxacin (2.5 mg/kg body weight, Baytril®; Bayer, Leverkusen, Germany) daily within the first three postoperative days. Sutures were removed 2 weeks later. No plaque-control program was initiated.

After 1, 2, 4 and 12 weeks of nonsubmerged implant healing, three animals were anaesthetized as described above. Afterwards, animals were sacrificed by inducing cardiac arrest with an intravenous injection of pentobarbital, 20% (w/v; Narcoren®; Merial, Hallbergmoos, Germany). Full-thickness mucosa samples were removed perpendicularly with a distance of 5 mm to the transmucosal implant part by means of a standardized scalpel biopsy. After dividing each sample perpendicularly into two equally sized parts, one half was stored in 4% formalin for histology/immunohistochemistry/immunofluorescence and the other one was stored in RNAlater™ (Ambion, Austin, TX, USA) for RT-PCR analysis. The tissue punch as well as the resected mucosa samples, obtained during implant placement, served as control.

Standard histology and histomorphometry

Formalin-fixed mucosa samples were embedded in paraffin (Histokinette, TP1020; Leica Biosystems, Nussloch, Germany) and cut into 4 µm vertical sections using the microtome (RM2145; Leica Biosystems). The sections were deparaffinized in xylene, rehydrated in a graded alcohol series and subjected to standard hematoxylin eosin staining as described previously [12]. Slides were examined quantitatively under a bright field microscope (Axioskop, Zeiss, Oberkochen, Germany) at ×200 original magnification. The number of transmigrated PMNs in the junctional epithelium was counted on three fields per section. The PMN is a very important cell in the first line defense against bacteria invasion. As bacteria populate, the sulcus PMNs are recruited and transmigrate the epithelium. The number of transmigrated PMNs is an indicator of the inflammatory status of the periimplant soft tissue. Additionally, the density of subepithelial inflammatory infiltration, which is another indicator for the degree of soft tissue inflammation, was semiquantified using a 10-cm visual analogue scale (VAS) with 0 representing loose and 10 very dense infiltration on three fields per section. Multiple counts/VAS values per section were aggregated prior to analysis. Comparison between the two groups at the different time points was made using the unpaired samples *t* test. Figures were presented as bar plots with mean and 2× standard deviation (SD). Two tailed *p* values ≤0.05 were considered

significant. All calculations were made using SPSS v15.0 for Windows (SPSS, Chicago, IL, USA).

Quantification of mRNA by real-time RT-PCR

Total RNA was extracted from periimplant mucosa using the RNeasy Mini Kit (QIAGEN, Hilden, Germany). RNA concentrations were determined spectrophotometrically (NanoDrop®, Wilmington, DE, USA). The mRNA of iNOS was semiquantified by RT-PCR employing the Rotor-Gene SYBR Green RT-PCR Kit (QIAGEN) and a Rotor-Gene Q Cycler system (QIAGEN). Inducible NOS is the marker enzyme of inflammatory macrophages, which are the predominant cell during the inflammatory phase of periimplant soft tissue healing. Consequently, iNOS tissue expression was determined as an indicator of duration and intensity of the inflammatory phase of wound healing. Assays were performed in 25 µl of reaction volume, which contained 12.5 µl of 2× Rotor-Gene SYBR Green RT-PCR Master Mix, 0.25 µl of Rotor-Gene RT Mix, 2.5 µl 10× QuantiTect Primer Assay primers (QIAGEN) for glyceraldehyde-3-phosphate dehydrogenase (GAPDH, QT00079247) or iNOS (QT00068740) and 10 ng/µl of total RNA. DNase-/Rnase-free water was added up to a total reaction volume of 25 µl in a 72-well Rotor. The PCR reaction cycles comprised 10 min at 55°C, 5 min at 95°C, followed by 40 cycles of 5 s at 95°C and 10 s 60°C.

Data were analyzed by the $\Delta\Delta$ -Ct method [13]. In brief, concentration in time (Ct) values of the genes of interest (iNOS) were corrected for Ct values from the housekeeping gene GAPDH, resulting in a Δ Ct value (Δ Ct=Ct_{iNOS}–Ct_{housekeeping gene (GAPDH)}}). $\Delta\Delta$ -Ct was calculated by subtracting the Δ Ct of the control group (unwounded oral mucosa) from the Δ Ct of the experimental group flapless or flap surgery ($\Delta\Delta$ Ct= Δ Ct_{experimental group}– Δ Ct_{control group}). Relative mRNA levels were calculated by $2^{-\Delta\Delta$ Ct} for each target gene. All reactions were performed in triplicate for each sample. Mean and SD were calculated for each group and each time point. Testing for group differences at the different time points was carried out using the unpaired samples *t* test. Figures were presented as bar plots with mean and SD. Two tailed *p* values ≤0.05 were considered significant. All calculations were made using SPSS v15.0 for Windows (SPSS, Chicago, IL, USA).

Immunofluorescence

Immunofluorescence staining was chosen to verify the vessels in the supracrestal connective tissue. The amount of vessels is proportional to the degree of inflammation on the one hand and reverses proportional to the degree of scarring of wounded tissue on the other hand. Consequently, vessels were investigated to get information about both inflamma-

tion and fibrosis. To eliminate unspecific binding, sections were blocked with 5% donkey serum for 30 min at room temperature. Sections were reacted with anti-CD 31 polyclonal-goat IgG antibody (1:100; Santa Cruz Biotechnology, Santa Cruz, CA, USA) for 60 min. Afterwards, sections were incubated with the secondary, Cy3-conjugated donkey anti-goat IgG (Jackson ImmunoResearch Laboratories, West Grove, PA, USA) at a 1:200 dilution for 30 min. Nuclei were counterstained with 4' 6-diamidino-2-phenylindole (DAPI, Sigma-Aldrich, Taufkirchen, Germany). Lastly, sections were mounted with Mowiol (Roth, Karlsruhe, Germany). Qualitative examination for size, distribution and density of vessels was performed at $\times 50$ –400 original magnification under the fluorescent microscope (Axioplan, Zeiss). The excitation wavelength for Cy3 was 550 nm. Red Cy 3 emission was selected and recorded by using a 570 nm rhodamine filter. In addition, DAPI was excited at 365 nm and its blue emission was recorded via a 420 nm DAPI filter. Photomicrographs of the regions of interest were taken using a CCD camera (Axiocam, Zeiss) and edited using Adobe Photoshop CS4 (Adobe Systems, Mountain View, CA, USA).

Immunohistochemistry

Biopsy specimens were subjected to immunohistochemical staining for collagen I using the avidin–biotin–peroxidase complex method as described previously [14]. In contrast to vessels, the density of collagen is reverse-proportional to inflammation and directly proportional to the degree of fibrosis. As with vessel density, collagen staining was performed to get information about inflammation and fibrosis of the periimplant soft tissue. Endogenous peroxidase was blocked by incubation in 3% H₂O₂ in methanol for 20 min. After the wash with tris-buffered saline (TBS), epitopes were demasked with trypsin solution (100 mg trypsin, 100 mg calcium chloride, TBS) at 37°C for 10 min. To eliminate nonspecific binding of antibodies, sections were incubated in 3% rabbit serum for 30 min at room temperature. Collagen I was marked with a polyclonal, unconjugated mouse IgG antibody (dilution 1:100; Santa Cruz Biotechnology, Billerica, MA, USA) at 4°C overnight and a polyclonal, biotinylated rabbit anti-mouse IgG (dilution 1:100; Dako, Glostrup, Denmark). For chromogenic development, avidin–biotin/horseradishperoxidase complex (ABC/HRP complex, BioFX Laboratories, Owings Mills, MD, USA) was used and DAB (Dako) served as a substrate. Cell nuclei were counterstained using Mayer's hematoxylin (Dako). Lastly, sections were dehydrated in a graded alcohol series and mounted with Eukitt (Sigma-Aldrich, Taufkirchen, Germany). Slides were examined qualitatively under a bright field microscope (Axioskop,

Zeiss, Oberkochen, Germany) at $\times 50$ –400 original magnification for extend and localization of collagen I fibers.

Results

Transmigration of inflammatory cells

In healthy unwounded mucosa, which was obtained from the tissue punch at the time of implant placement, a mean number of nine transmigrated PMNs/visual field (SD: five cells/visual field) was counted. Over the entire investigation period, the number of transmigrated PMNs was significantly higher for the flap surgery group as compared with the flapless surgery group (Fig. 1).

Density of subepithelial inflammatory infiltrates

In healthy unwounded mucosa, a mean density of inflammatory infiltrates of 2.6 VAS points (SD: 1.3 VAS points) was reached. A significantly higher density of subepithelial inflammatory infiltrates was found following flap surgery as compared with the flapless technique 1, 2, 4 and 12 weeks post-surgery (Fig. 2).

Expression of iNOS

Relative iNOS expression was 0.6 (SD: 0.5) in the healthy unwounded mucosa. Over the investigation period, iNOS

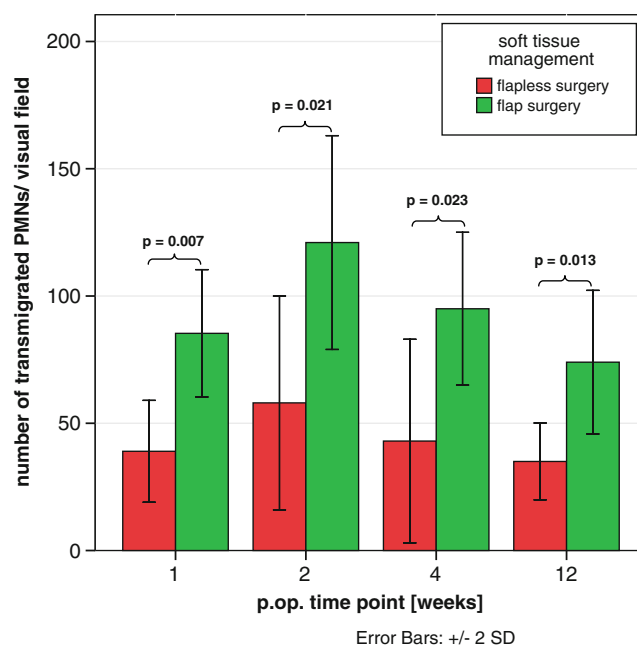


Fig. 1 Bar plot showing the number of transmigrated PMNs/visual field at $\times 200$ original magnification over the entire investigation period as a function of the soft tissue management at the time of implant insertion. Bars means, error bars $\times 2$ SD

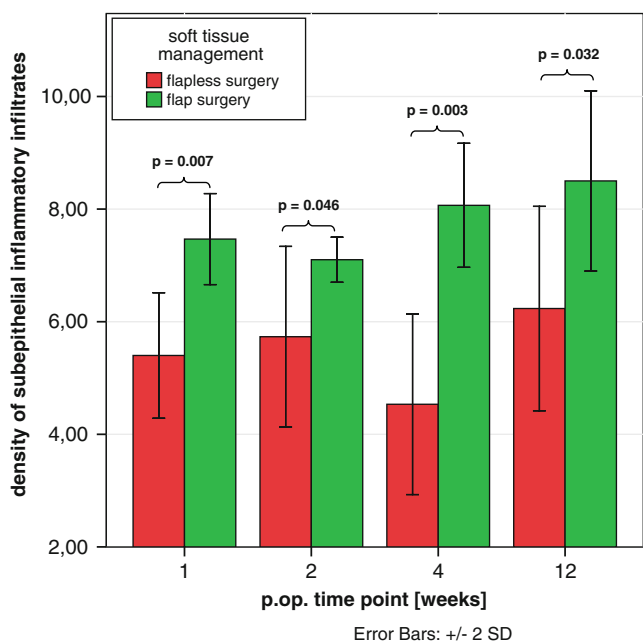


Fig. 2 Bar plot showing the density of the subepithelial inflammatory infiltrates as visual analogue scale value (0...very loose infiltration until 10...dense infiltration) over the entire investigation period as a function of the soft tissue management at the time of implant insertion. Bars means, error bars 2× SD

expression was higher following flap surgery as compared with flapless surgery. This difference reached statistical significance 2, 4 and 12 weeks post-surgery (Fig. 3).

Collagen I (COL I)

While no differences in the collagen architecture were observable between both groups 1 and 2 weeks post-insertion, a reduction in collagen density was observable for the flap surgery group 4 and 12 weeks post-insertion (Fig. 4).

Perfusion

Over the entire investigation period, CD31-positive vessels were found to be homogeneously distributed in the supra-crestal connective tissue following flapless surgery. After flap surgery, a more spot-like distribution was noticeable. No differences in the diameter of the vessels were found between the groups. Furthermore, vessel density was higher following flapless placement as compared with the flap approach 4 and 12 weeks post-insertion (Fig. 5).

Discussion

Taking into account the lack of knowledge regarding the influence of the insertion technique on the incidence of

periimplant mucositis and periimplantitis [6], it was the aim of the present study to investigate signs of periimplant infectious lesions during a time period of 3 months as a function of soft tissue management during implant insertion.

Over the entire investigation period, flap surgery resulted in a significantly larger transmigration of inflammatory cells, density of subepithelial, inflammatory infiltration and iNOS expression as compared with flapless placement. Hypothesis 1 was confirmed by the data. This periimplant inflammatory infiltration has three different sources: (1) periimplant wound healing [12, 15], (2) inflammation elicited by the suturing material [16] and (3) periimplant infection due to plaque accumulation [17].

The inflammatory phase of wound healing can be subdivided in an early and late response. The early phase lasts for 48–72 h and is characterized by tissue infiltration with PMNs, which are recruited as a first-line defense against infection [18]. At the time of first biopsy retrieval, the early response has already progressed into the late inflammatory response with the macrophage being the key cell. The monocyte/macrophage is drawn to the wound by chemoattractants such as transforming growth factor-β, platelet-derived growth factor and various complement cascade components [19]. The wound macrophage has many roles in wound healing, with one of the important functions being prevention of infection and removal of debris by releasing reactive oxygen species, like nitric oxide, which is produced from L-arginine by the iNOS. As

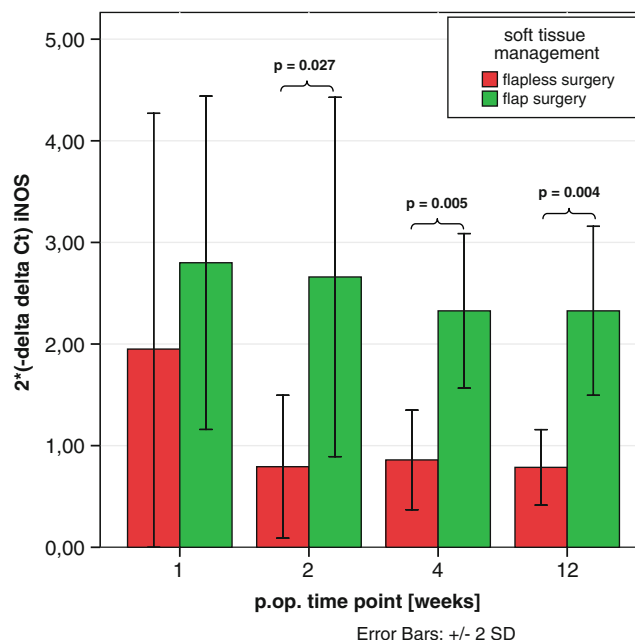
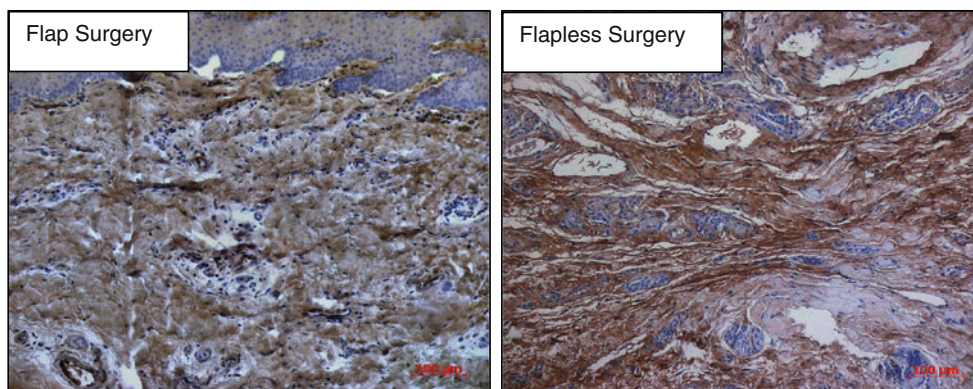


Fig. 3 Bar plot showing the relative expression of iNOS over the entire investigation period as a function of the soft tissue management at the time of implant insertion. Bars means, error bars 2× SD

Fig. 4 Representative sections of immunohistochemical collagen I staining in the supracrestal connective tissue 4-weeks post-insertion



it is known that the intensity of the elicited wound healing response is a direct function of the amount of tissue trauma [15, 20], reduced surgical trauma following flapless placement partially explains the observed differences between both groups. Fibroblasts become the dominant cell type by 10 days post-wounding and the inflammatory response turns into the proliferative phase of wound healing [21]. Consequently, differences in the wound healing response elicited by the surgical trauma do not longer explain the observed intergroup differences.

In our study, suturing employing monofil, non-absorbable nylon (3–0 Ethilon) was performed in the flap surgery group. Berdahl et al. tested nylon as suturing material in a chicken model and found inflammatory host responses to the material [22, 23]. Sutures were removed 2 weeks post-insertion. Consequently, inflammation elicited by the suturing material might partially contribute to increased inflammation in the flap surgery group.

Additionally, according to the concepts of inflammatory periodontal disease progression published by Page and Schroeder [17], an early gingivitis lesion might be present as soon as 1 week post-insertion and develop into an established lesion until week 4 due to undisturbed plaque accumulation. This lesion might be more pronounced in the flap surgery group due to the larger wound surface, which allows for increased bacteria invasion. Furthermore, the enhanced reepithelization [12], reduced length of the

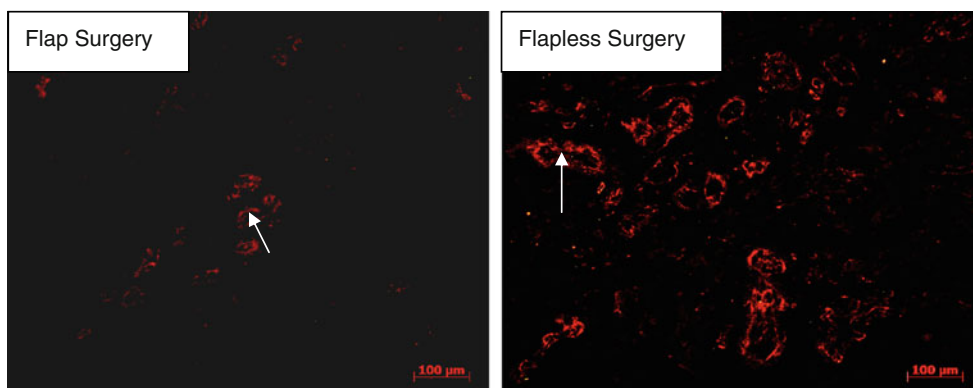
junctional epithelium [7] and increased number of blood vessels [8] in the supracrestal connective tissue following flapless placement might provide a more effective barrier against bacterial invasion then in the flap surgery group.

Four and 12 weeks post-implantation, a reduced collagen as well as vessel density were determined in the flap surgery group. Hypothesis 2 was confirmed by the data. The reduction in collagen density might be due to the sustained presence of large amounts of inflammatory cells [17]. Those cells are thought to change the periimplant microenvironment by secretion of cytokines (e.g. interferon- γ ; tumor necrosis factor- α ; interleukin (IL)-1 α/β ; IL-6; IL-10; IL-12; IL-13), chemokines, matrix metalloproteinases and prostaglandin E2. IL-1 β enhances the production of collagenase in gingival and desmodontal fibroblasts and reduced collagen synthesis. PGE2 reduces collagen synthesis in gingival fibroblasts [24].

Conclusion

The data of the present study indicate that flapless placement reduces the incidence of inflammatory periimplant soft tissue lesions during a 12-week period and thus might improve the long-term stability of dental implants. Considering the beneficial effects of flapless placement on early soft tissue healing and stability, the technique might

Fig. 5 Representative sections of immunofluorescent CD 31 staining for detection of vessels (*white arrows*) in the supracrestal connective tissue 4 weeks post-insertion



be preferred in case of an uncomplicated locoregional anatomy with sufficient hard and soft tissue. However, this positive effect might disappear after manipulation of the implant and soft tissue during impression-taking or try in of the prosthodontic supraconstruction.

Acknowledgements The authors are grateful to Dr. Harald Schubert (Institute for Experimental Animals, University of Jena) for providing help with the animal experiments as well as Maia Mtsariashvili for performing the RT-PCR as well as histology. The study was supported by grants of the Interdisciplinary Center for Clinical Research (IZKF) at the University Hospital Jena as part of the research cooperation 4.

Conflict of interest statement The authors declare that they have no conflict of interest.

References

- Choi BH, Engelke W (2009) “Flapless Implantology”—Möglichkeiten und Grenzen. *Implantologie* 17:139–152
- Kan JY, Rungcharassaeng K, Ojano M, Goodacre CJ (2000) Flapless anterior implant surgery: a surgical and prosthodontic rationale. *Pract Periodontics Aesthet Dent* 12:467–474
- Hammerle CH, Stone P, Jung RE, Kapos T, Brodala N (2009) Consensus statements and recommended clinical procedures regarding computer-assisted implant dentistry. *Int J Oral Maxillofac Implants* 24(Suppl):126–131
- Fortin T, Bosson JL, Isidori M, Blanchet E (2006) Effect of flapless surgery on pain experienced in implant placement using an image-guided system. *Int J Oral Maxillofac Implants* 21:298–304
- Cannizzaro G, Leone M, Esposito M (2008) Immediate versus early loading of two implants placed with a flapless technique supporting mandibular bar-retained overdentures: a single-blinded, randomized controlled clinical trial. *Eur J Oral Implantol* 1:33–43
- Esposito M, Grusovin MG, Maghaireh H, Coulthard P, Worthington HV (2007) Interventions for replacing missing teeth: management of soft tissues for dental implants. *Cochrane database of systematic reviews (Online)* (3):CD006697
- You TM, Choi BH, Li J, Xuan F, Jeong SM, Jang SO (2009) Morphogenesis of the peri-implant mucosa: a comparison between flap and flapless procedures in the canine mandible. *Oral Surg Oral Med Oral Pathol Oral Radiol Endod* 107:66–70
- Kim JI, Choi BH, Li J, Xuan F, Jeong SM (2009) Blood vessels of the peri-implant mucosa: a comparison between flap and flapless procedures. *Oral Surg Oral Med Oral Pathol Oral Radiol Endod* 107:508–512
- Jeong SM, Choi BH, Li J, Kim HS, Ko CY, Jung JH, Lee HJ, Lee SH, Engelke W (2007) Flapless implant surgery: an experimental study. *Oral Surg Oral Med Oral Pathol Oral Radiol Endod* 104:24–28
- Jeong SM, Choi BH, Li J, Ahn KM, Lee SH, Xuan F (2008) Bone healing around implants following flap and mini-flap surgeries: a radiographic evaluation between stage I and stage II surgery. *Oral Surg Oral Med Oral Pathol Oral Radiol Endod* 105:293–296
- Rimondini L, Bruschi GB, Scipioni A, Carrassi A, Nicoli-Aldini N, Giavaresi G, Fini M, Mortellaro C, Giardino R (2005) Tissue healing in implants immediately placed into postextraction sockets: a pilot study in a mini-pig model. *Oral Surg Oral Med Oral Pathol Oral Radiol Endod* 100:e43–e50
- Mueller CK, Thorwarth M, Schultze-Mosgau S (2010) Influence of insertion protocol and implant shoulder design on inflammatory infiltration and gene expression in peri-implant soft tissue during nonsubmerged dental implant healing. *Oral Surg Oral Med Oral Pathol Oral Radiol Endod* 109:e11–e19
- Livak KJ, Schmittgen TD (2001) Analysis of relative gene expression data using real-time quantitative PCR and the 2^{(-Delta Delta C(T))} method. *Methods (S Diego, Calif)* 25:402–408
- Schultze-Mosgau S, Rodel F, Radespiel-Troger M, Worl J, Grabenbauer GG, Neukam FW (2002) Vascularization of the area between free grafts and irradiated graft beds in the neck in rats. *Brit J Oral Maxillofac Surg* 40:37–44
- Schultze-Mosgau S, Blatz MB, Wehrhan F, Schlegel KA, Thorwart M, Holst S (2005) Principles and mechanisms of peri-implant soft tissue healing. *Quintessence Int* 36:759–769
- Arcuri C, Cecchetti F, Dri M, Muzzi F, Bartuli FN (2006) Suture in oral surgery. A comparative study. *Min Stomatol* 55:17–31
- Page RC, Schroeder HE (1976) Pathogenesis of inflammatory periodontal disease. A summary of current work. Laboratory investigation. *J Techn Meth Pathol* 34:235–249
- Kwon DH, Bisch FC, Herold RW, Pompe C, Bastone P, Rodriguez NA, Susin C, Wikesjo UM (2010) Periodontal wound healing/regeneration following the application of rhGDF-5 in a beta-TCP/PLGA carrier in critical-size supra-alveolar periodontal defects in dogs. *J Clin Periodontol* 37:667–674
- Beanes SR, Dang C, Soo C, Ting K (2003) Skin repair and scar formation: the central role of TGF-beta. *Exp Rev Mol Med* 5:1–22
- Schultze-Mosgau S, Kopp J, Thorwarth M, Rodel F, Melnychenko I, Grabenbauer GG, Amann K, Wehrhan F (2006) Plasminogen activator inhibitor-I-related regulation of procollagen I (alpha1 and alpha2) by antitransforming growth factor-beta1 treatment during radiation-impaired wound healing. *Int J Radiat Oncol Biol Phys* 64:280–288
- Nygaard-Ostby P, Bakke V, Nesdal O, Susin C, Wikesjo UM (2010) Periodontal healing following reconstructive surgery: effect of guided tissue regeneration using a bioresorbable barrier device when combined with autogenous bone grafting. A randomized-controlled trial 10-year follow-up. *J Clin Periodontol* 37:366–373
- Berdahl JP, Johnson CS, Proia AD, Grinstaff MW, Kim T (2009) Comparison of sutures and dendritic polymer adhesives for corneal laceration repair in an in vivo chicken model. *Arch Ophthalmol* 127:442–447
- Andrade MG, Weissman R, Reis SR (2006) Tissue reaction and surface morphology of absorbable sutures after in vivo exposure. *J Mat Sci* 17:949–961
- Mueller CK, Schultze-Mosgau S (2009) Radiation-induced micro-environments—the molecular basis for free flap complications in the pre-irradiated field? *Radiother Oncol* 93:581–585

Copyright of Clinical Oral Investigations is the property of Springer Science & Business Media B.V. and its content may not be copied or emailed to multiple sites or posted to a listserv without the copyright holder's express written permission. However, users may print, download, or email articles for individual use.